

A Comparative Analysis between Unbiased Exponential Resummation and Taylor Expansion in Finite-Density QCD with a new phasefactor for Isospin

Sabarnya Mitra^{a,b}

^a *Centre for High Energy Physics, Indian Institute of Science, Bengaluru 560012, India*

^b *Fakültat Für Physik, Universität Bielefeld 33615, Germany*

E-mail: smitra@physik.uni-bielefeld.de, sabarnyam@iisc.ac.in

ABSTRACT: The recently introduced unbiased exponential resummation at finite chemical potential has become an important approach which promises to capture reliably the behaviour of higher order conserved charge cumulants appearing otherwise in the finite-density QCD Taylor series of thermodynamic observables. In this paper, we present a thorough analysis of the estimates of charge cumulants upto eighth order and have compared them using Taylor expansion method and unbiased exponential resummation approach for baryon and isospin chemical potentials. We also subsequently compare the different estimates of the radius of convergence obtained using these two methods and check if the zeros of phasefactor for baryochemical potential can indicate something about these estimated values. We propose a new method of finding a non-trivial phasefactor for isospin chemical potential and we attempt explaining the different estimates of radius of convergence from the zeroes of this newly constructed gauge-ensemble average phasefactor for isospin chemical potential. Lastly, we also illustrate kurtosis plots describing the behaviour of overlap problem in isospin chemical potential and check if it maintains consistency with the appearance of zeros of the newly proposed phasefactor.

Contents

1	Introduction	1
2	Taylor expansion and Unbiased exponential resummation	3
2.1	Taylor Expansion	4
2.2	Unbiased Exponential Resummation	4
2.3	Unbiased formalism	5
2.4	Idea of complex isospin chemical potential and associated phasefactor	6
3	Overlap problem and its severity	6
4	Setup of calculations	7
5	Results	9
5.1	For baryon chemical potential	9
5.2	For isospin chemical potential	15
6	Conclusions	18

1 Introduction

The strong force, one of the four fundamental forces of Nature is very well described by the quantum field theory of Quantum Chromodynamics (QCD) [1]. An immensely important and intriguing spectacle in the paradigm of these strong interactions is the QCD phase diagram which features various interesting phases of strongly interacting matter. One of the important aspects of QCD is to explore and map this phase diagram [2–5] as a function of temperature T and baryochemical potential μ_B . This is pivotal not only for understanding the strong dynamics at various energy scales, but also for illuminating the physics of early universe [6, 7]. Despite being very robust and seemingly self-explanatory, most of this phase diagram have been constructed out from mere symmetry arguments and analyses of various QCD models. They continue to remain conjectured and await further conclusive evidences. In the quest of such evidences, one often resorts to formulating QCD on a lattice of spacetime [8, 9] mostly because of its remarkable ability to successfully predict results to appreciable degree of precision. Besides offering possible signatures of unexplored phases, the non-perturbative formulation of thermodynamics in lattice QCD also enables one to obtain significant insights about the phase diagram. Like at present, lattice simulations can well explain the manifestations at finite temperature, zero μ_B which resembles the vertical axis of the phase diagram. It also establishes that the phase transition between the hadronic phase and the quark-gluon plasma phases at zero μ_B is an analytical crossover [10–14].

However for real finite μ_B , lattice QCD faces a stumbling block in the shape of sign problem [15–18]. At finite μ_B , the path integral [19] expressing the QCD partition function Z becomes complex with its measure containing a complex fermion determinant [20] which gives rise to the problem of complex measure. This complex measure hinders implementation of Monte-Carlo importance sampling for estimating this path integral. While reweighting [21, 22] this complex measure with a real fermion determinant at zero μ_B makes the measure real, the observable part of the integral becomes complex which, after Monte-Carlo estimation provides a phaseangle θ and a subsequent phasefactor $\cos \theta$ for every gauge configuration of the working ensemble. The severity of this sign problem is governed by the magnitude of this $\cos \theta$ averaged over the entire ensemble, the value of which decreases towards zero for higher values of μ_B thereby reflecting increasing severity of the sign problem. This happens because the integrand exhibits tremendous oscillations across positive and negative real values, each of which is also large in magnitude, causing the mean to settle towards zero. This sign problem eventually leads to the breakdown of lattice QCD computations at a finite value of μ_B reflected by the non-monotonic behaviour of the calculated observables. This highly restricts our investigation and consequent knowledge of QCD at finite density.

Several new methods [23–29] have been introduced which can successfully avoid this sign problem, most of which unfortunately have very limited applications in QCD explicitly. In the case of QCD, the Taylor expansion around $\mu_B = 0$ [30–35] and analytic continuation of simulations from imaginary to real μ_B [36–38] continue to remain the prominent methods for circumventing the sign problem and providing state-of-the-art results for QCD equation of state [39–47] at finite μ_B . Resummation approaches like Padé [48–50] and exponential resummation [51] have been proposed, to improve the slowly convergent Taylor series results. While the former approximates the Taylor coefficients by rational functions where one is interested to find the roots and poles of these functions, the latter provides a direct estimate of Z in the form of an exponential in which the argument comprises finite contributions of lower order Taylor series. Recently, the new formalism of unbiased exponential resummation [52, 53] has been introduced for obtaining a more improved QCD Equation of state at finite chemical potential, by obviating the stochastic bias [54] and reproducing the exact Taylor series to a given order in μ , where μ is any generic flavor of chemical potential. This unbiased approach [55] is paramount for recognising the genuine higher order Taylor contributions captured through this approach of resummation.

Although the breakdown of calculations can be detected by observing the onset of the zeros of phasefactor for μ_B , it is not the case for μ_I since it has no sign problem. Hence, it is not possible to identify a possible breakdown in μ_I by looking for the zeros of the phasefactor, which never becomes zero. Although this means that in principle, one can perform unbiased exponential resummation to all real values of μ_I extending to infinity, studies suggest that there is a genuine phase diagram [56–59] in the $T - \mu_I$ plane which illustrates the formation of a pion condensate starting from some finite value of μ_I for a low T . This signifies that at a low T surely, this formalism is supposed to have a finite radius of convergence in μ_I and is expected to experience a breakdown beyond that. Apart from many other objectives, this paper tries to come up with a new indicator for this purpose.

The paper is organised as follows: In Section 2, we provide a quick overview about the Taylor expansion and the unbiased exponential resummation formalism, which constitute the two main cornerstone of comparisons in this paper. This is accompanied by a brief description about phasefactor of this resummation formalism, and the new idea of a complex phasefactor which is being proposed to identify possible breakdown for μ_I . In Section 3, we have discussed briefly about the overlap problem and its severity along μ_I . Starting from the details of scale setting and setup of lattice including random volume sources and gauge configurations used in constructing the Taylor coefficients, the method of error estimation for unbiased exponential resummation formalism are highlighted in Section 4. In Section 5, we present vivid discussions regarding the comparisons between the sixth and eighth order conserved charge cumulants for both μ_B and μ_I obtained from Taylor expansion and unbiased exponential resummation. We also demonstrate the same for the different estimates of the radius of convergence, and attempt to observe if the onset of zeros of the gauge ensemble averaged phasefactor $\langle \cos \theta \rangle$ and complex phasefactor $\langle e^{i\theta} \rangle$ can provide indications consistent with these estimates of radius of convergence for μ_B and μ_I respectively. Because if this happens, they can then provide consistent indications about the start of breakdown for μ_B and μ_I . In the last part of this section, we illuminate the behaviour of overlap problem in μ_I and see if this is consistent with the implications made by the zeros of phasefactor and their onset in μ_I . We have concluded the paper and its discussion by providing a brief summary in Section 6. Throughout this paper, we have used relativistic units ($\hbar = c = 1$) and unit Boltzmann constant, and have often denoted μ/T as μ . Often we have used this notation μ in this paper to imply both μ_B and μ_I .

2 Taylor expansion and Unbiased exponential resummation

In a $2 + 1$ flavor QCD with staggered rooted quarks, the grand-canonical partition function Z with suppressed volume dependence for a given temperature T and chemical potential μ is given as

$$Z(T, \mu) = \int \mathcal{D}U e^{-S_G[T, U]} \det \mathcal{M}(T, \mu, U) \quad (2.1)$$

with the fermionic determinant $\det \mathcal{M}(T, \mu, U)$ being

$$\det \mathcal{M}(T, \mu, U) = \prod_{f=u,d,s} [\det \mathcal{M}(T, \mu_f, U)]^{1/4} \quad (2.2)$$

In the above Eqns.(2.1) and (2.2), U represent the gauge field configurations and functional $S_G[T, U]$ denotes the gluon action. For a thermodynamic system of volume V at temperature T , the excess pressure $\Delta P(T, \mu)$ is given as follows:

$$\frac{\Delta P(T, \mu)}{T^4} = \frac{P(T, \mu) - P(T, 0)}{T^4} = \frac{1}{VT^3} \ln \left[\frac{Z(T, \mu)}{Z(T, 0)} \right] \quad (2.3)$$

This measure of excess pressure in Eqn.(2.3), scaled in powers of T is dimensionless which makes it useful for calculations at finite temperature on a given lattice.

2.1 Taylor Expansion

The Taylor Expansion of this excess pressure to $\mathcal{O}(\mu^N)$ is given by

$$\frac{\Delta P_N^T(T, \mu)}{T^4} = \sum_{n=1}^{N/2} \frac{\chi_{2n}}{(2n)!} \left(\frac{\mu}{T}\right)^{2n} \quad (2.4)$$

where in the above Eqn.(2.4), χ_{2n} is the conserved charge cumulant of order $2n$. The n^{th} Taylor coefficient is defined as $c_n = \chi_n/n!$. The CP symmetry of QCD instructs this Taylor series of Eqn.(2.4) to be even in μ which implies that N is even. In terms of the different correlation functions D_n where the n^{th} order correlation function D_n is defined as

$$D_n(T) = \left. \frac{\partial^n \ln \det \mathcal{M}(T, \mu)}{\partial \mu^n} \right|_{\mu=0} \quad (2.5)$$

the first four χ_n can be expressed as follows:

$$\begin{aligned} \chi_1 &= \langle D_1 \rangle \\ \chi_2 &= \langle D_2 \rangle + \langle D_1^2 \rangle \\ \chi_3 &= \langle D_3 \rangle + 3 \langle D_2 D_1 \rangle + \langle D_1^3 \rangle \\ \chi_4 &= \langle D_4 \rangle + 4 \langle D_3 D_1 \rangle + 3 \langle D_2^2 \rangle + 6 \langle D_2 D_1^2 \rangle + \langle D_1^4 \rangle \end{aligned} \quad (2.6)$$

Throughout this paper, the notation $\langle \mathcal{O} \rangle$ represents Monte-Carlo sampling average of observable \mathcal{O} over all gauge configurations in the ensemble generated at $\mu = 0$. All these powers are necessarily the unbiased powers of the respective D_n .

2.2 Unbiased Exponential Resummation

Exponential Resummation

The method of exponential resummation commences with estimating the partition function directly and then deducing the thermodynamic quantities successively following the subsequent thermodynamic relations. In this approach, the ratio $Z(T, \mu)/Z(T, 0)$ in the above Eqn.(2.3) to $\mathcal{O}(\mu^N)$ is given by

$$Z_N^R(T, \mu) \equiv \frac{Z(T, \mu)}{Z(T, 0)} = \left\langle \exp \left(\sum_{n=1}^N \left(\frac{\mu}{T}\right)^n \frac{D_n}{n!} \right) \right\rangle \quad (2.7)$$

with the symbols having conventional meanings as explained above. On an isotropic¹ lattice of size $N_\sigma^3 \cdot N_\tau$ in 3+1 spacetime having N_σ points in each of the 3 spatial directions and N_τ points in the temporal direction, the estimate of excess pressure for exponential resummation is obtained as follows:

$$\frac{\Delta P_N^R(T, \mu)}{T^4} = \left(\frac{N_\tau}{N_\sigma} \right)^3 \ln Z_N^R(T, \mu) \quad (2.8)$$

¹In isotropic lattice, spatial spacing a_σ = temporal spacing a_τ .

where the expression of Z_N^R is given in the above Eqn.(2.7). The partition function Z for any real μ is real-valued by virtue of the CP symmetry of QCD. which makes the D_n given in Eqn.(2.5) real or imaginary for even or odd n respectively.

Stochastic Bias

However since the fermion matrix \mathcal{M} cannot be evaluated exactly using analytical means [60], these correlation functions D_n require numerical estimation. This is done by considering a finite number of random volume sources for every gauge configuration and thereby estimating D_n for every random source for each gauge configuration. Hence in this limit, D_n of Eqn.(2.7) is replaced by \overline{D}_n , which is given as:

$$\overline{D}_n = \frac{1}{N_R} \sum_{r=1}^{N_R} D_n^{(r)} \quad (2.9)$$

Here in Eqn.(2.9), $D_n^{(r)}$ is the estimate of D_n in the r^{th} random volume source and N_R is the total number of such random volume sources. One also needs to extract the real part of this complex exponential in Eqn.(2.7) for determining the estimate of Z_R^N preserving the CP symmetry of QCD. In this limit, the above Eqn.(2.7) therefore resembles

$$Z_N^R = \text{Re} \left\langle \left[\exp \left(\sum_{n=1}^N \left(\frac{\mu}{T} \right)^n \frac{\overline{D}_n}{n!} \right) \right] \right\rangle \quad (2.10)$$

where \overline{D}_n is provided in Eqn.(2.9). Using finite N_R results in stochastic bias in usual exponential resummation formula as well as provides biased estimates of different D_n for every gauge configuration. A detailed description about this stochastic bias can be found in Ref.[54]. Although this bias decreases as N_R^{-1} , it can be very significant depending on the observable probed and the value and order of μ under consideration. It becomes highly imperative to eliminate this bias which can hinder genuine transparent understanding of underlying physics for finite-density QCD.

2.3 Unbiased formalism

The unbiased exponential resummation is formulated to eliminate this stochastic bias. In this formalism, the original structure of the resummation is retained with subtle modification of the argument of exponential. This is done so that on expansion in μ , it produces unbiased estimates of D_n and thereby reproduces Taylor series exactly to a given order in μ . This is true for any flavor of chemical potential, although we have implemented this for μ_B and μ_I in this paper. For both μ_B and μ_I , the unbiased formalism provides the following expression of the excess pressure $\Delta P/T^4$:

$$\begin{aligned} \frac{\Delta P_N^u(T, \mu)}{T^4} &= \frac{1}{VT^3} \ln Z_N^u(T, \mu) \quad \text{where} \\ Z_N^u(T, \mu) &= \text{Re} \left\langle \left[\exp \left(\sum_{n=1}^N \left(\frac{\mu}{T} \right)^n \frac{\overline{D}_n^u}{n!} \right) \right] \right\rangle \end{aligned} \quad (2.11)$$

The above Eqn.(2.11) resembles Eqn.(2.10) with the notable exception that in the unbiased formalism, the argument of exponential in the expression of the unbiased partition function Z_N^u comprises the unbiased estimates \overline{D}_n^u of D_n as the coefficient of μ^n . A detailed proof along with other mathematical details of this formalism are presented in [52].

2.4 Idea of complex isospin chemical potential and associated phasefactor

The formalism of exponential resummation provides another significant entity which is the phasefactor. The gauge ensemble averaged phasefactor reflects the degree of μ -dependent oscillations of $\det \mathcal{M}$. Close to the zeros of this average phasefactor, the oscillations become highly severe and may often lead to breakdown of calculations, rendering the formalism unreliable. Thus the manifestation of these zeros and their onset are interesting since they can provide a good estimate about the commencement of a possible breakdown. As mentioned regarding Eqn.(2.10), the exponential of the complex polynomial comprising purely real (imaginary) D_n for even (odd) values of n yield a complex exponential. So for a complex function $z(T, \mu)$, this can be written as $e^z = R e^{i\theta}$ where

$$R(T, \mu) = \exp \left[\text{Re} \left(z(T, \mu) \right) \right], \theta(T, \mu) = \text{Im} \left[z(T, \mu) \right]$$

In the case of μ_B , the exponential is complex for real values of μ_B and since one needs to extract the real part of the exponential, the phasefactor in this case is given by $\cos \theta$ for every gauge configuration. Hence in this situation we compute and observe the behaviour of $\langle \cos \theta \rangle$ as a function of μ_B .

However for μ_I , the exponential is always real for real μ_I since D_n vanishes for odd n . Since $\theta(T, \mu)$ ² only depends on odd D_n , hence $\theta = 0$ for every gauge configuration for μ_I , making $\cos \theta = 1$. This makes identifying the breakdown in case of μ_I difficult by inspecting the behaviour of $\langle \cos \theta \rangle$ for real μ_I , just like μ_B . In this paper, we propose to make μ_I complex which will make the resummation exponential complex. This will then provide us with a non-trivial phasefactor which will vary for various μ_I spanning the complex μ_I plane. Since CP symmetry does not guarantee partition function to be real for complex values of chemical potential, we observe the behaviour of the entire complex phasefactor $\langle e^{i\theta} \rangle$ for complex μ_I as opposed to observing just $\langle \text{Re}(e^{i\theta}) \rangle = \langle \cos \theta \rangle$ for real μ_B . The two dimensional phasefactor plots for μ_I have been constructed in this paper, by plotting the absolute value of $\langle e^{i\theta} \rangle$ i.e. $|\langle e^{i\theta} \rangle|$ as a function of $|\mu_I|$.

3 Overlap problem and its severity

In this section, we give a brief introduction to the overlap problem that becomes pre-dominant in computations involving real μ_I . Despite the absence of sign problem in μ_I , the calculations experience a genuine breakdown beyond a finite radius of convergence ρ .

While generating an ensemble of fermion and gauge field configurations at finite μ_I based on extrapolations from the ensemble generated at $\mu_I = 0$, this problem arises when

$$^2\theta(T, \mu) = \sum_{n=1}^N \left(\frac{\mu}{T} \right)^{2n-1} \text{Im}(D_{2n-1})$$

the distribution or sample comprising the ratio of fermion determinants at finite μ_I to zero μ_I i.e. $\det \mathcal{M}(\mu_I)/\det \mathcal{M}(0)$ becomes heavily tailed. This large tail of the distribution causes Monte-Carlo importance sampling ineffective, and renders reweighting approach inefficient in this limit. One comes across this ratio while reweighting the integrand of the path integral given in Eqn. (2.1), and this ratio assumes different values for different gauge configuration ensembles. In the realm of reweighting and exponential resummation where $|\mu_I| < \rho$, this ratio for a gauge configuration U can be expressed as

$$\frac{\det \mathcal{M}(\mu_I, U)}{\det \mathcal{M}(0, U)} = \exp \left[\sum_{n=1}^{\infty} \mu_I^n \frac{D_n(U)}{n!} \right], \quad D_n(U) = \frac{\partial^n}{\partial \mu_I^n} \ln \det \mathcal{M}(\mu_I, U) \Big|_{\mu_I=0} \quad (3.1)$$

The volume and temperature dependence of fermion determinant have been suppressed in the above Eqn. (3.1), for the given gauge configuration U . These values of the above ratio for a given μ_I and for all such U in the ensemble constitute the working sample or distribution and its tail characterises the magnitude and extent of overlap problem. A heavily tailed distribution³ will have greater extent of overlap problem. This is because in these distributions, the values radically different from the distribution mean, manifest with appreciable probability and this trait tends to change the sample statistics by a large extent. Although standard deviation can prove to be a reliable estimate characterising the heavy tail, a better quantitative measure is kurtosis κ which is the standardised fourth order central moment. For a total of N gauge field configurations, this is represented by:

$$\kappa(\mu_I) = \frac{M_4^{\bar{x}}(\mu_I)}{(\sigma(\mu_I))^4} \quad (3.2)$$

where $M_4^{\bar{x}}$ is the fourth order central moment and σ is the standard deviation of the distribution with mean \bar{x} . These are defined as

$$M_4^{\bar{x}} = \frac{1}{N} \sum_{i=1}^N (x_i - \bar{x})^4, \quad \sigma = \left[\frac{1}{N} \sum_{i=1}^N (x_i - \bar{x})^2 \right]^{\frac{1}{2}}, \quad \bar{x} = \frac{1}{N} \sum_{i=1}^N x_i \quad (3.3)$$

where $x_i = [\det \mathcal{M}(\mu_I)/\det \mathcal{M}(0)]_i$ is the value of the fermion determinant ratio obtained from i^{th} configuration. The manifestation of this overlap problem however may be different for different formalism which are adopted suitably for subsequent calculations for probing finite density QCD regime.

4 Setup of calculations

In this work, we have extensively used the data generated by the HotQCD collaboration for its ongoing Taylor expansion calculations and charge fluctuations. We discuss the setup and other important relevant details of this data, in this section.

³These distributions have large sample variance and often the sample mean is drastically different from the population mean.

The QCD action considered for generating the working data of the calculations in this work follows a $2 + 1$ flavor signature in which the strange quark is 27 times more massive than the mass degenerate up and down quarks. This action comprises a Symanzik-improved gauge action [61, 62] and the Highly Improved Staggered Quark (HISQ) fermion action [63–65]. Gauge field configurations of order $\mathcal{O}(10^4 - 10^6)$ are generated in the temperature range $135 \text{ MeV} \lesssim T \lesssim 176 \text{ MeV}$ with $N_\tau = 8, 12$ and 16 and $N_\sigma = 4N_\tau$. In this work, an isotropic lattice of size $32^3 \cdot 8$ has been used in Euclidean four spacetime, which is Wick rotated from the usual $3 + 1$ relativistic Minkowski spacetime. Following the relation $T = (aN_\tau)^{-1}$, the temperature for each N_τ is varied by varying the isotropic lattice spacing a through the inverse gauge coupling⁴ β . For each a , the bare light and strange quark masses $m_l(a)$ and $m_s(a)$ are also tuned so that the pseudo-Goldstone pion and kaon masses produced become equal to the physical pion (π) and kaon (K) masses respectively. This fixes the line of constant physics for the lattice setup under consideration. The scale setting is determined using both the Sommer parameter r_1 and the kaon decay constant f_K . A complete description of the gauge ensembles and scale setting is provided in Ref. [66].

To calculate the charge cumulants for unbiased exponential resummation, the baryon and isospin correlation functions D_1, \dots, D_6 are estimated stochastically using 500 Gaussian volume sources on each gauge configuration. For a detailed derivation of these D_n , refer to [67]. The exponential- μ formalism is used to calculate the first four correlation functions, and further higher derivatives are calculated using the linear- μ formalism. This is because the ultraviolet divergences remain upto fourth power of μ_B or μ_I and in order to take care of it, the complete formula of these correlation functions must be considered in which besides the linear trace term, one also takes into account the traces involving non-linear μ derivatives of fermion matrix \mathcal{M} . Using this data, we have calculated the necessary results which are to be discussed vividly in the next section for μ_B and μ_I using the methods of Taylor expansion and unbiased exponential resummation. These are computed in the range $0 \leq |\mu_{B,I}/T| \leq 2.5$, using $100K$ configurations for μ_B and $20K$ configurations per temperature for μ_I . More statistics have been used for μ_B over μ_I because the sign problem in the former tends to lower the signal-noise ratio. Our results have been obtained on $N_\tau = 8$ lattices for three temperatures namely at $T \sim 135, 157$ and 176 MeV . Besides describing the hadronic, crossover and QGP phases of QCD phase diagram, these temperatures have been chosen carefully as being approximately equal to T_{pc} and $T_{pc} \pm 20 \text{ MeV}$, where $T_{pc} = 156.5(1.5) \text{ MeV}$ is the chiral crossover temperature at zero baryon chemical potential μ_B for physical values of bare quark masses [68]. The same temperatures have been chosen as the working temperatures for μ_I also.

In all these calculations involving Taylor expansion and unbiased exponential resummation, we have considered taking 100 bootstrap samples of the working gauge configuration ensemble. This bootstrapping algorithm used, is based on a chosen random number generator and is implemented to calculate the errorbars associated with values of the observables, computed in this paper.

⁴ $\beta = 6/g^2$ where g is the QCD coupling parameter.

5 Results

5.1 For baryon chemical potential

In this section, we present a comparative study between the measures of baryon cumulants of sixth and eighth orders obtained using the usual Taylor Expansion and the measures of the same that appear on expansion of the unbiased exponential resummation formula. The Taylor coefficients⁵ using the Taylor expansion are procured from the different unbiased powers of the corresponding baryon or isospin correlation functions, as given in Eqn.(2.6). As mentioned before, the manifestation of the stochastic bias has already been observed in the old exponential resummation formula [51] and not only we have understood the importance of eliminating this bias [54], we also have come up with the unbiased exponential resummation [52] which replicates the exact Taylor coefficients corresponding to the appropriate powers of μ . Thus within its all-order series, it reproduces Taylor series upto a desired order in μ which leads to a more improved QCD Equation of state and enabling one to comprehend the true physics of finite-density QCD, to a more reliable extent.

The higher order charge cumulants or coefficients, are particularly of great significance. Owing to the higher powers of μ associated with these coefficients, their values strongly influence the behaviour of Taylor series for larger values of μ ($\mu/T > 1$), which is instrumental for understanding finite-density QCD. From a computational point of view, it is very difficult and expensive to evaluate these higher order Taylor coefficients as they require calculating higher order correlation functions and also the higher unbiased powers of the required lower-order correlation functions. So, it is very challenging to evaluate these Taylor coefficients precisely and therefore would be promising if they can be ascertained using some other alternative means, from which they can be obtained with similar precision at the expense of relatively less computational complexities. In this paper, we attempt to testify this using unbiased exponential resummation of second and fourth orders for finite μ_B and μ_I and compare the subsequent results between these two approaches.

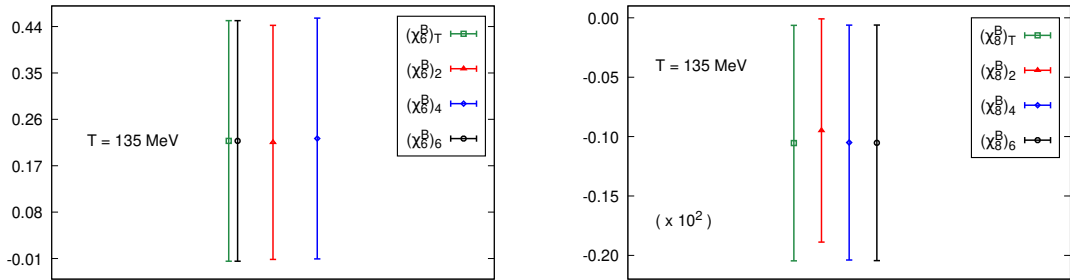


Figure 1. Plots of sixth and eighth order baryon cumulants χ_6^B (left) and χ_8^B (right) obtained using the Taylor expansion and also from the unbiased exponential resummation of second, fourth and sixth orders at $T = 135 \text{ MeV}$. The green points indicate the usual Taylor estimate of the cumulants whereas the red, blue and black lines represent the same for second, fourth and sixth orders respectively.

⁵Taylor coefficient is just the charge cumulant scaled by appropriate factorial.

Fig.1 represents the plots of χ_6^B and χ_8^B obtained using the usual Taylor Expansion method and the unbiased exponential resummation approach. The $(\chi_n^B)_T$ depicts the estimate of χ_n^B acquired using Taylor expansion, whereas $(\chi_n^B)_m$ represents the same procured from the unbiased exponential resummation of order m , in which correlation functions only upto order m are being taken into account. The subsequent plots in this paper follow this nomenclature of symbols only, even for the plots of μ_I in the later section of the paper. As mentioned before while estimating $(\chi_n^B)_m$, all the correlation functions from D_1 to D_m are included and all the higher correlation functions starting from D_{m+1} are ruled out. It is therefore very evident that the sixth order unbiased exponential resummation contains all the necessary unbiased powers of D_n upto $n = 6$ and hence in principle, $(\chi_6^B)_6 = (\chi_6^B)_T$ (Eqn.(2.6)). This is clearly demonstrated in the left plot of Fig.1 where the green and the black lines representing respective $(\chi_6^B)_T$ and $(\chi_6^B)_6$ matches exactly, with the errorbars also in perfect alignment with each other. Strictly speaking, this argument holds true for all the charge cumulants having the order less than the order of the unbiased resummation. In mathematical terms, this implies $(\chi_n^B)_T = (\chi_n^B)_m$ for all $m \geq n$. This is vividly observed from the following Fig.2 where we find the measure of χ_2 is exactly identical for all the orders of unbiased resummation and is equal to the corresponding Taylor estimate $(\chi_2^B)_T$. We also observe that as expected, the estimate of χ_4 differs from $(\chi_4^B)_T$ only for second order resummation calculations. They agree exactly with the Taylor result that is, $(\chi_4^B)_T$ from fourth order onwards in terms of both the mean values and errorbars.

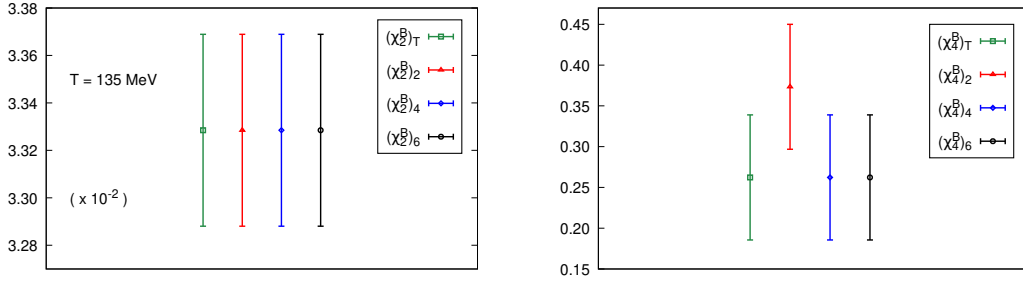


Figure 2. Plots of second and fourth order baryon cumulants χ_2^B (left) and χ_4^B (right) obtained using the Taylor expansion and also from the unbiased exponential resummation of second, fourth and sixth orders at $T = 135$ MeV. The color and symbol nomenclature remains the same.

Fig.1 clearly illustrates that the measurements of χ_8^B exhibit stochastic fluctuations to a much greater extent, as compared to χ_6^B . This is expected as the determination of higher order charge cumulants require evaluating higher order D_n^B , more number of diagrams and also higher values of unbiased powers, all of which eventually contribute to the larger magnitudes of these fluctuations. This is very evident from the larger errorbars for χ_8^B in the right plot compared to χ_6^B in the left plot of Fig.1. Although this difference is almost of the order of 10^2 , we find that the resummation estimates align well with the corresponding Taylor estimates for both χ_6^B and χ_8^B at this temperature. We also observe from this figure that unlike the second order unbiased resummation estimates shown by the red points, the estimates of χ_6 and χ_8 obtained from the fourth and sixth order unbiased resummation

(blue and black points) remain more or less in an appreciable agreement with $(\chi_6^B)_T$ and $(\chi_8^B)_T$ respectively, where these Taylor results are illustrated by the green points.

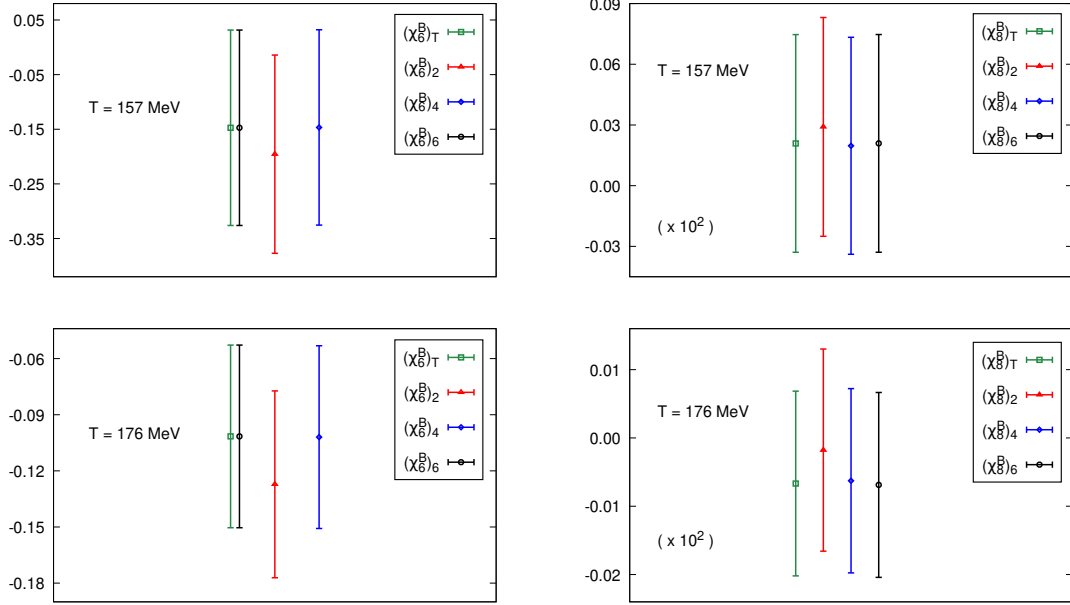


Figure 3. Plots of sixth and eighth order charge cumulants χ_6^B (left column) and χ_8^B (right column) obtained using the Taylor expansion and also from the unbiased exponential resummation of second, fourth and sixth orders. These are obtained at 157 (top row) and 176 MeV (bottom row) respectively, with the same meaning of symbols and colors.

Similar sort of argument holds true also for the other two temperatures, namely at 157 and 176 MeV respectively as shown in the Fig.3. As compared to Fig.1, the difference between the second order resummation estimates and the corresponding Taylor estimates increases for higher temperatures at 157 and 176 MeV. This is demonstrated in Fig.3, where we find a considerable inequality between $(\chi_n^B)_2$ and $(\chi_n^B)_T$ for $n = 6, 8$. This may be caused by the increasing magnitude of the remaining higher order terms or diagrams with temperature, which contribute to the Taylor calculation but not in the second order resummation estimate thereby leading to larger differences. Despite this, we observe that the fourth and sixth order resummation estimates, $(\chi_n^B)_6$ and $(\chi_n^B)_8$ continues to remain in a good agreement with the corresponding Taylor estimates. Although there are some differences, these are much less as compared to $(\chi_n^B)_2$ and we also find for $n = 6, 8$, the mean values and errorbars $(\chi_n^B)_4$ and $(\chi_n^B)_6$ are well-aligned with $(\chi_n^B)_T$ as shown by the blue and black points in Fig.3.

It is important to note one interesting feature of this set of observations. Although the second order resummation estimates vary a lot from the Taylor estimates, the difference becomes perceptibly small from fourth order onwards and both the mean values as well as the associated errorbars of the resummation calculations seem to agree well with the Taylor counterparts. This holds true for all the four charge cumulant measurements at all

the three working temperatures namely 135, 157 and 176 MeV which represent hadronic, crossover and plasma phases of the QCD phase diagram for physical quark and pion masses. This may seemingly suggest that the calculation of unbiased estimates upto D_4 for μ_B or equivalently upto $\mathcal{O}(\mu_B^4)$ and thereafter performing exponential resummation may be good enough to reproduce Taylor series upto $\mathcal{O}(\mu_B^8)$ irrespective of whether or not, the stochastic bias from D_5 is taken care of. The question of whether this remains valid for even higher powers of μ_B beyond μ_B^8 is certainly a very interesting work for the future and if found true, will have huge benefits by reducing computational work and time, to a great extent.

Apart from the estimates of these individual charge cumulants, we also compare and present results regarding the different estimates of the radius of convergence obtained from the Taylor expansion and the unbiased exponential resummation method. The radius of convergence of a Taylor series determines the value of the parameter of expansion (μ in this case) upto which the series approximation provides reliable results and hence, it is also significant for identifying the possible breakdown of calculations which use Taylor series approximations. As stated before due to the CP symmetry or particle-antiparticle symmetry of QCD, the Taylor series of QCD excess pressure (see Eqn.(2.4)) is even in $\mu \equiv \mu_B/\mu_I$ for which the radius of convergence ρ in principle is given by

$$\rho = \lim_{n \rightarrow \infty} \rho_n, \text{ where } \rho_n = \sqrt{\frac{c_{2n}}{c_{2n+2}}} \quad (5.1)$$

In Eqn.(5.1), $c_n = \chi_n/n!$ is the n^{th} order Taylor coefficient appearing Taylor expansion of excess pressure. Although the radius of convergence is in principle, mentioned mostly in the context of Taylor series, we have measured the different estimates of this radius of convergence ρ in the case of unbiased exponential resummation too. This is possible because on expansion of this resummed series in terms of μ , it resembles a Taylor series in μ whose resulting coefficients differ from the usual Taylor coefficients. This depends on the argument of the exponential of the resummation formula which in turn is dependent on the resummation order. In this work, this has been done by considering the unbiased resummation to second, fourth and sixth orders in μ_B and subsequently measuring the appropriate charge cumulants χ_n of different orders n , before determining ρ using Eqn.(5.1).

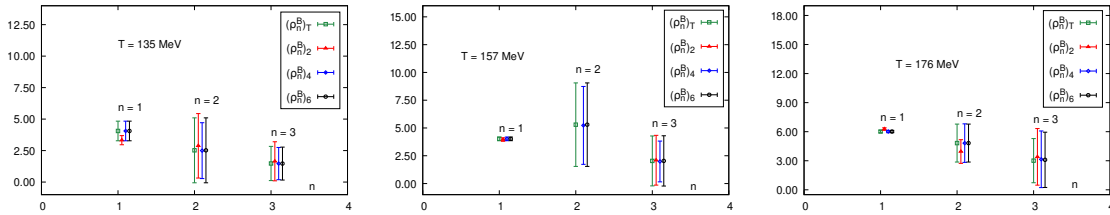


Figure 4. Plots of the estimate of $\rho_n = \sqrt{(c_{2n}/c_{2n+2})}$ with $n = 1, 2, 3$ for μ_B obtained at 135 (left), 157 (center) and 176 MeV (right). The green line represents the Taylor estimate of the radius of convergence whereas the red, blue and black lines depict the same for unbiased exponential resummation approach upto second, fourth and sixth orders in μ_B respectively.

In this work, we have measured three estimates of the radius of convergence using this

unbiased exponential resummation. These estimates are ρ_1 , ρ_2 and ρ_3 which are obtained by inserting $n = 1, 2, 3$ in the Eqn.(5.1). Since the highest order Taylor series used in this work is of eighth order, the best and most reliable estimate of radius of convergence is $\rho_3 = (c_6/c_8)^{1/2}$. In terms of charge cumulants χ , the three estimates are as follows:

$$\rho_1 = \sqrt{12 \frac{\chi_2}{\chi_4}} , \quad \rho_2 = \sqrt{30 \frac{\chi_4}{\chi_6}} , \quad \rho_3 = \sqrt{56 \frac{\chi_6}{\chi_8}} \quad (5.2)$$

In Fig.4, we have presented plots illuminating these different estimates of ρ as given in Eqn.(5.2). The different estimates ρ_1, ρ_2 and ρ_3 of the radius of convergence have been plotted at 135, 157 and 176 MeV respectively. The green points depict the Taylor estimates whereas the red, blue and the black points illustrate the estimates obtained using unbiased exponential resummation of second, fourth and sixth orders respectively. As mentioned before, these estimates have been compared after obtaining them using the Taylor expansion approach and also through the method of unbiased exponential resummation for second, fourth and sixth orders in μ_B . It is very evident from the previous discussion regarding charge cumulants χ_n that $(\rho_1^B)_T = (\rho_1^B)_n$ for $n = 4, 6$. This is because, determination of ρ_1^B requires knowledge of χ_2^B and χ_4^B , each of which can be completely known to its Taylor estimate from unbiased exponential resummation of fourth order onwards. Similarly in the case of ρ_2 , one should expect in principle that $(\rho_2^B)_T = (\rho_2^B)_n$ for $n = 6$ only and should not be identical to $(\rho_2^B)_2$ or $(\rho_2^B)_4$. The determination of ρ_3^B is interesting in this case, because in order to calculate χ_8^B to its Taylor counterpart (see Eqn.(5.2)), one should be needing eighth order unbiased resummation. Being lower than eighth order, all the three orders of unbiased resummation used in this paper are expected to exude some differences over the Taylor estimate $(\rho_3^B)_T$ in the determination of ρ_3^B .

All this set of theoretical expectations are exactly satisfied in Fig.4. It is clearly observed that while all the colored points are differently positioned at $n = 3$ for all the three temperatures, the black points merge with the green points for $n = 2$ indicating that $(\rho_2^B)_T = (\rho_2^B)_6$. Also for $n = 1$, both the blue and black points completely overlap with the green points depicting $(\rho_1^B)_T = (\rho_1^B)_4 = (\rho_1^B)_6$, and this is true for all the three working temperatures. We clearly find that there is a noticeable distinction between the Taylor estimates shown in green points and the second order unbiased resummation estimates shown by the red points. The Taylor expansion data used has been verified to satisfy that ρ_1^B is minimum and ρ_2^B is maximum at 157 MeV.

On a general note, the second order resummation estimates shown in the form of red points exhibit most of the deviation from the corresponding Taylor estimates. This happens for all the three working temperatures, specially for ρ_1 and ρ_2 . Although the second order resummation estimate for ρ_2 remains somewhat consistent with the Taylor and the resummation estimates of other orders at 135 and 176 MeV, it diverges away completely at 157 MeV and that is why, it also cannot be captured in the central plot of Fig.4. This happens as χ_4^B attains a maximum and χ_6^B attains a minimum at 157 MeV which is the crossover or the pseudo-critical temperature for the physical values of the quark masses, thereby causing ρ_2 to offshoot (see Eqn.(5.2)). Despite this, we also find that most of these deviations happen for the measurements of ρ_1 and ρ_2 only. While estimating ρ_3

which should supposedly be the best estimate of these three estimates, we observe that the resummation estimates of all the second, fourth and sixth orders exhibit consistency and remain in good agreement with one another and the corresponding Taylor estimate. Although there are some differences, these differences are expected as discussed above and even after taking them into account, we clearly observe that they are not dramatically different from what the Taylor results provide us. A detailed study of the values and errorbars would surely be an interesting work for the future.

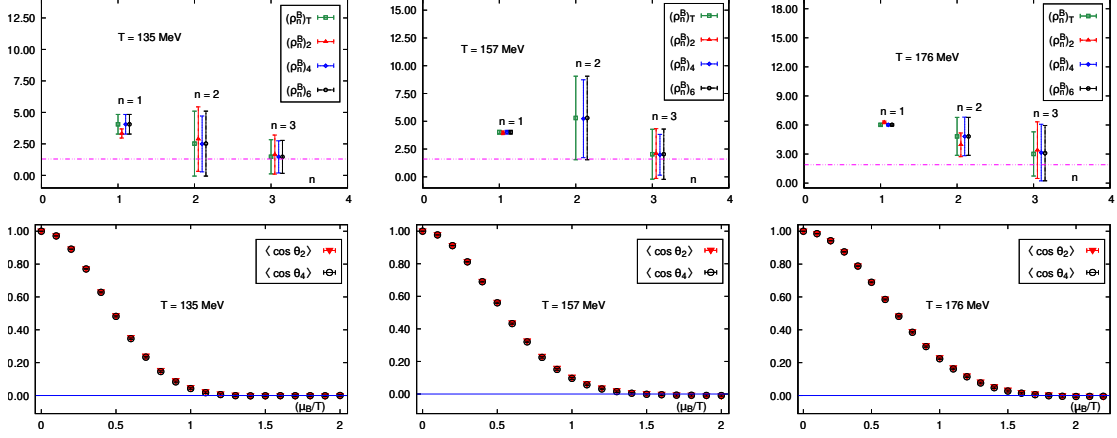


Figure 5. (Top row) Plots of ρ_1^B, ρ_2^B and ρ_3^B at 135 (left), 157 (middle) and 176 MeV (right) respectively. (Bottom row) Plots of $\langle \cos \theta \rangle$ as a function of μ_B/T for second and fourth order unbiased resummation plotted at 135 (left), 157 (middle) and 176 MeV (right) respectively. The red and black points in the phasefactor plots illustrate $\langle \cos \theta \rangle$ obtained from unbiased resummation performed upto second and fourth orders in μ_B respectively. The blue line in the phasefactor plots indicates the zero line whereas the magenta line in the top row plots illustrate the value of μ_B/T from where $\langle \cos \theta \rangle = 0$.

We also present our observations regarding the behaviour of the gauge ensemble averaged phasefactor $\langle \cos \theta \rangle$ as a function of μ_B in Fig.5, and subsequently check if the onset of the zeros of this phasefactor coincide with values of estimates of the radius of convergence obtained which can help identifying the start of the breakdown of calculations. As introduced before, this phasefactor is $e^{i\theta}$ whose real part $\cos \theta$ needs to be analysed for μ_B since the partition function is real for real μ_B . This is obtained from the unbiased exponential resummation and we find that the red and black points in the plots of the lower row of Fig.5 indicate the average phasefactor value procured from unbiased resummation to second order and fourth order respectively. The blue line in the lower row plots is the zero line of the phasefactor, which ascertains the value of μ_B from where $\langle \cos \theta_n \rangle$ becomes zero for $n = 2, 4$. This value of μ_B is illustrated by the magenta dotted line in the upper row plots of the same Fig.5. From this figure, it is explicitly observed that the zeros of $\langle \cos \theta \rangle$ for both the second and fourth orders of unbiased resummation agree very well with each other and also become zero starting from the same value of μ_B . This remains valid despite this value of μ_B being different for different working temperatures. Even though the dotted line in magenta does not coincide with the estimates of ρ_1^B for

all the temperatures and becomes non-coincident with ρ_2 for $T = 157$ and 176 MeV, it coincides well with the estimates of ρ_3 for all the three working temperatures at 135, 157 and 176 MeV. This is positive and encouraging, as this implies that the onset of zeros of $\langle \cos \theta \rangle$ obtained using unbiased exponential resummation upto fourth order only, can very well indicate the estimated radius of convergence of the Taylor series. This is because we have already discussed that ρ_3^B is the most reliable estimate of the radius of convergence among all these three estimates, and so this demonstrates that the onset of the zeros of $\langle \cos \theta \rangle$ can provide reliable indications about the estimate of radius of convergence leading to subsequently reliable signs about the onset of breakdown in μ_B .

5.2 For isospin chemical potential

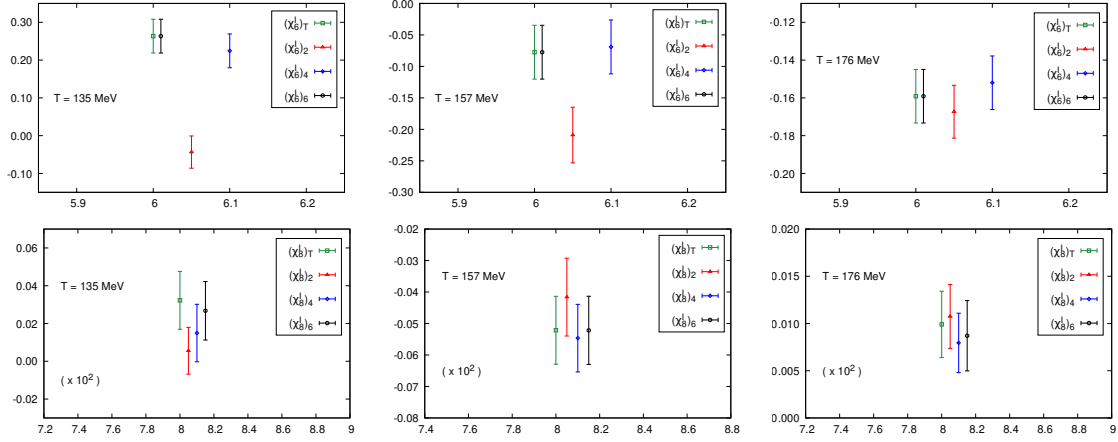


Figure 6. Plots for the isospin cumulants χ_6^I (top row) and χ_8^I (bottom row) obtained from the methods of Taylor expansions and unbiased exponential resummation. These are obtained for 135 (left column), 157 (middle column) and 176 MeV (right column) respectively with the same color and symbol nomenclature.

In this section, we present the same results for isospin chemical potential μ_I . The comparison regarding χ_6 and χ_8 is illustrated for all the three working temperatures in Fig.6. However as compared to μ_B we find from Fig.6, the resummation estimates differ a lot from the Taylor counterparts. The second order resummation estimate departs the most from the Taylor results whereas the degree of deviation reduces on considering higher orders of unbiased resummation. This difference between $(\rho_n^I)_T$ and $(\rho_n^I)_2$ for $n = 6, 8$ is maximum at 135 MeV and reduces with increasing temperature. Unlike μ_B , we find that the fourth order resummation estimate show some differences with the corresponding Taylor estimate in the determination of χ_8^I .

This may happen because firstly, the odd order isospin correlation functions vanish unlike μ_B . In case of μ_B , most of these odd order correlation functions would appear with a negative sign and would tend to nullify the contributions of even order correlation functions coming with a positive sign. An exact reason of this nature of sign still needs to be ascertained. Moreover, we also found that the different even order isospin correlation

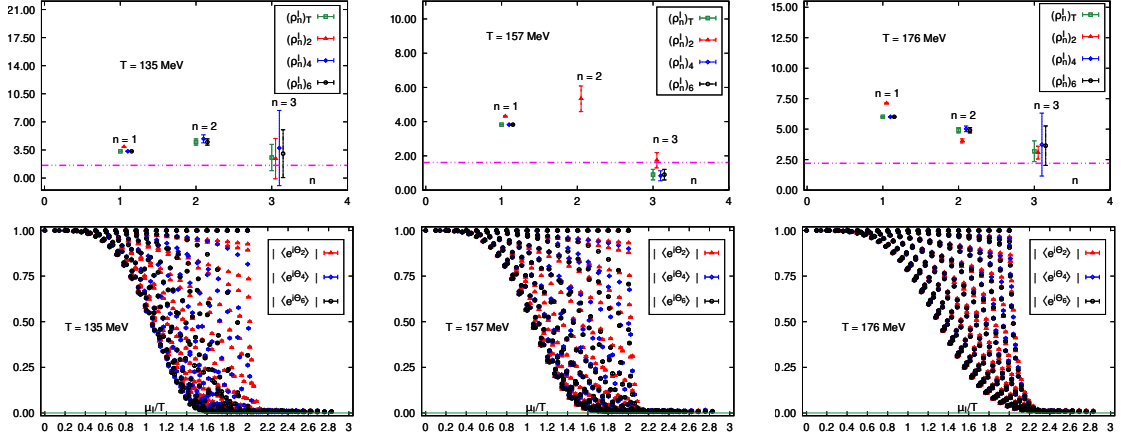


Figure 7. (Top row) Plots of ρ_1^I, ρ_2^I and ρ_3^I at 135 (left), 157 (middle) and 176 MeV (right) respectively. (Bottom row) Plots of $\langle e^{i\theta} \rangle$ as a function of μ_I/T for second, fourth and sixth order unbiased exponential resummation plotted at 135 (left), 157 (middle) and 176 MeV (right) respectively. The red, blue and black points in these bottom row plots depict $\langle e^{i\theta} \rangle$ of unbiased resummation to second, fourth and sixth orders in μ_I/T respectively, whereas the magenta line in the top row plots illustrate the value of μ_I/T manifesting the onset of $\langle e^{i\theta} \rangle = 0$.

functions are much greater than baryon correlation functions of similar orders, and this difference increases with temperature and for higher orders and unbiased powers. As a consequence, the contribution of higher order correlation functions D_6 and D_8 get highly enhanced in case of μ_I , for which taking unbiased powers only upto μ_I^4 and performing unbiased exponential resummation is not enough to replicate eighth order Taylor series in μ_I . In the case of μ_B , the higher order contributions of D_6^B and D_8^B do not offshoot like μ_I and hence, we observe that the agreement between Taylor and resummation estimates become appreciable from fourth order onwards for all the three working temperatures as shown in Fig.1.

Just like μ_B , we have also plotted the different estimates of radius of convergence in Fig.7 for μ_I and compared these estimates obtained from the Taylor expansion and unbiased exponential resummation approaches. These different estimates ρ_1^I, ρ_2^I and ρ_3^I have been plotted in the upper row of this figure, with the symbols following the nomenclature as mentioned before. Despite having some appreciable differences between the Taylor and unbiased resummation estimates at the level of individual charge cumulants, the estimates of the radius of convergence exhibit some signs of agreement. Although it is observed that the second order resummation estimates shown in red points exhibit appreciable discrepancies with the Taylor results specially at 135 and 157 MeV, the estimates obtained from the fourth and sixth orders unbiased resummation comply to a commendable extent and show appreciable consistency with the corresponding Taylor estimates.

In this paper, we have formulated a new way of evaluating a non-trivial phasefactor for μ_I and just like μ_B , we have checked if this new formulation of the average phasefactor can provide reliable indications about the radius of convergence and possible breakdown in the case of μ_I . These phasefactor plots have been constructed in the bottom row of this figure.

Unlike μ_B , we have determined a complex phasefactor $e^{i\theta}$ in the case of μ_I . The trick is to make the isospin chemical potential μ_I complex and from the consequent complex reweighting factor, compute the gauge ensemble average $\langle e^{i\theta} \rangle$ and observe its behaviour for various complex μ_I . This is because for real μ_I the phasefactor is unity for all the gauge configurations due to vanishing odd-order isospin correlation functions and thereby, cannot be used as an indicator for identifying breakdown of calculations. As mentioned before, the partition function can become complex and does not have to be real for complex chemical potentials, and so this allows one to have a non-trivial phasefactor since the phaseangle becomes non-zero and varies with the value of complex μ_I .

In this paper, we have traced two-dimensional plots of ⁶ $|\langle e^{i\theta} \rangle|$ as a function of $|\mu_I|$ as demonstrated in the bottom row plots of Fig.7. $|\mu_I|$ is the radial distance of the complex μ_I from the origin in the complex μ_I plane. This is beneficial in the sense that $|\mu_I|$ is identical to μ_I along the real axis and it also provides us a new way of exploring the behaviour of phasefactor along real μ_I . We have also computed the phasefactor from sixth order resummation for μ_I since unlike μ_B , we observed a very appreciable agreement in the estimates of the isospin cumulants χ_6^I and χ_8^I between the Taylor results and the sixth order unbiased exponential resummation. Unlike Fig.5, there is a possibility of having multiple points of phasefactor for a given μ_I/T ⁷ in the phasefactor plots of μ_I in Fig.7 and hence as we observe, there are more number of points as compared to μ_B . However unlike μ_B , we find that not all the phasefactor points coincide with the zero phasefactor line at a particular value of μ_I . Rather we observe that with increasing value of μ_I , the phasefactor points start going towards the zero phasefactor line and different points coincide with this line at different values of μ_I , until from a given value all the phasefactor points stack and settle on this zero line, similar to Fig.5 for the case of μ_B . Despite this, we clearly notice that all the three orders of unbiased resummation do consistently provide the first zeros of $|\langle e^{i\theta} \rangle|$ at almost the same value of μ_I . These first zeros are important and should be noted as these are the very zeros which mark the beginning of increasing fluctuations of fermionic determinant causing $|\langle e^{i\theta} \rangle| = 0$. These values of μ_I for 135, 157 and 176 MeV at which these first zeros appear, are illustrated by the dotted magenta line in the upper row plots of Fig.7. We need to check if these first zeros can give some sort of indications about the radius of convergence and subsequent breakdown. The phasefactor has been calculated using unbiased resummation upto sixth order and has been plotted for 135, 157 and 176 MeV respectively.

We clearly sight from Fig.7 that the magenta line is far from coinciding with the estimates ρ_n^I for $n = 1, 2$ at all the three working temperatures. This is not very concerning, as the best estimate in this case is ρ_3^I since it takes into account the highest order charge cumulant χ_8^I . We observe that though the first zeros appear far away from ρ_1^I and ρ_2^I , they are very near to coinciding with ρ_3^I for all these three temperatures. Although the zeros start appearing beyond the estimate of ρ_3^I at 157 MeV, they are consistent and within errorbars of the individual estimates, are in good agreement with ρ_3^I at 135 and 176

⁶ $|\langle e^{i\theta} \rangle| = \sqrt{\langle \cos \theta \rangle^2 + \langle \sin \theta \rangle^2}$

⁷ This is because $x + iy$ and $y + ix$ will have same value of μ_I/T , but can have different values of $\langle e^{i\theta} \rangle$.

MeV. Thus, the point of the first appearance of zeros of $|\langle e^{i\theta} \rangle|$ procured using second and fourth order unbiased resummation approaches, provides commendable indications about the radius of convergence and the possible breakdown at least for eighth order Taylor series. This is somewhat promising, although the agreement with the same is not so well-defined at 157 MeV. We may have to look out for some other indicators of radius of convergence at this temperature. It may also signify that maybe in order to capture the genuine behaviour of the Taylor series at 157 MeV, it is important to go to even higher-than-eighth order calculations or it may also require the determination of unbiased phasefactor from a higher-than-sixth-order unbiased exponential resummation.

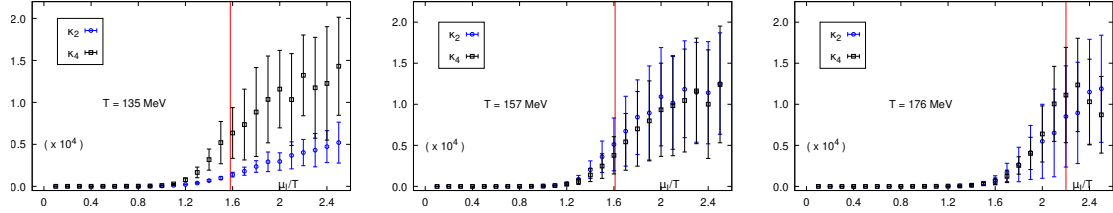


Figure 8. Plots of second and fourth order kurtosis κ_2 and κ_4 as a function of μ_I/T for 135 (left), 157 (center) and 176 MeV (right). The blue and black points illustrate the second and fourth order kurtosis and the red vertical line illustrates the point of first zero of $\langle e^{i\theta} \rangle$ as shown above in Fig.7.

Lastly, we also present results manifesting the behaviour of kurtosis as a function of μ_I/T . The kurtosis offers a quantitative measure of the overlap problem and its severity, which have been briefly discussed before. This overlap problem becomes visibly predominant for μ_I where there is no sign problem, and maybe the most possible reason for a breakdown. In Fig.8, we observe that both the second and fourth order kurtosis exhibits a monotonically increasing behaviour for higher values of μ_I . This is expected since the extent of overlap between distributions generated at finite μ_I and zero μ_I reduces with increasing value of the finite μ_I , and is evident from the higher values of the associated errorbars as seen in Fig.8. The red vertical line depicts the appearance of first zero of $\langle e^{i\theta} \rangle$, which coincides with the value of magenta line shown in Fig.7 as mentioned before. Fig.8 demonstrates that for all the three temperatures, the errorbars increase rapidly across this red line. This indicates that as the oscillations of the complex fermionic determinant for complex μ_I increases making $\langle e^{i\theta} \rangle \approx 0$, the overlap problem rapidly increases. Apart from the increasing errorbars, this is also manifested by the non-monotonic behaviour of the second and fourth order kurtosis values. This is an encouraging sight as one can understand the severity of this overlap problem and associated breakdown by studying the behaviour of this newly proposed complex phasefactor and observing the value of μ_I at which its first zero manifests.

6 Conclusions

In this paper, we have conducted a detailed comparative study between the estimates of higher order charge cumulants, namely χ_6 and χ_8 for both μ_B and μ_I which have

been obtained using the approaches of Taylor expansion and the unbiased exponential resummation. The estimates of these cumulants are exact in Taylor expansion, in the sense that all the necessary and appropriate correlation functions have been included with proper estimation of their unbiased powers before averaging them over the working gauge ensemble. On the other hand, correlation functions only upto order N are kept in N^{th} order unbiased exponential resummation and it is only from these non-zero correlation functions in this approach that the respective charge cumulants of sixth and eighth orders are evaluated and estimated.

Although there still remains a lot to investigate and scope for further progress, it has been evident from the aforementioned results that for μ_B , the resummed estimates of the sixth and eighth order charge cumulants seem to give excellent agreement with the corresponding Taylor estimates. More importantly, this commendable compatibility and agreement between the estimates of these two approaches is achieved for all the working temperatures from unbiased exponential resummation of fourth order onwards. However, this is not completely true for μ_I where we find that there are some discrepancies between the fourth order resummation estimate and the Taylor estimate for χ_8^I , which are considerably reduced when one performs this resummation to sixth order in μ_I . This is also the very reason why the isospin phasefactor has been calculated and procured from sixth order unbiased exponential resummation. A detailed study behind this discrepancy and other important features is certainly a work for future. We also have computed and compared the various estimates of radius of convergence between these two formalisms. We have observed that except the second order resummation, the fourth and sixth order resummation estimates agree very well with the corresponding Taylor estimate for all the working temperatures for both μ_B and μ_I .

We have also investigated the zeros of the gauge-ensemble average phasefactor and found that the zeros in case of μ_B provide promising indications of radius of convergence of Taylor series and subsequent breakdown. Apart from μ_B , this also holds true to some extent for μ_I where we have proposed a new formula for a non-trivial phasefactor by considering complex μ_I . Except 157 MeV, we found that the first zeros of this newly formulated phasefactor align very well with the estimate of ρ_3^I for 135 and 176 MeV and therefore can offer with some degree of reliability, promising indications about the onset of breakdown of calculations and also the estimate of radius of convergence of the associated Taylor series. At the end, we also demonstrated the nature of the overlap problem with μ_I and illustrated that the onset of the zeros of this newly proposed phasefactor is more or less consistent with this problem and this overlap problem becomes severely large, with excessively high errorbars and non-monotonic behaviour beyond the point of these first zeros, for all the three working temperatures.

Acknowledgments

I sincerely acknowledge Prasad Hegde and Frithjof Karsch for highly useful discussions and stimulating constructive suggestions for this draft. I also sincerely thank all the other members of the HotQCD collaboration for their inputs and valuable insights, as well as

for allowing me to use their data for the respective Taylor expansion calculations. The computations in this work have been performed on the GPU cluster at Bielefeld University, Germany. I also heartily thank the Bielefeld HPC.NRW team for their wholehearted support.

References

- [1] F. Gross et al., *50 Years of Quantum Chromodynamics*, [2212.11107](#).
- [2] M.A. Halasz, A.D. Jackson, R.E. Shrock, M.A. Stephanov and J.J.M. Verbaarschot, *Phase diagram of qcd*, *Phys. Rev. D* **58** (1998) 096007.
- [3] K. Rajagopal, *Mapping the QCD phase diagram*, *Nucl. Phys. A* **661** (1999) 150 [[hep-ph/9908360](#)].
- [4] M.A. Stephanov, *QCD phase diagram: An Overview*, *PoS LAT2006* (2006) 024 [[hep-lat/0701002](#)].
- [5] K. Fukushima and T. Hatsuda, *The phase diagram of dense qcd*, *Reports on Progress in Physics* **74** (2010) 014001.
- [6] M. McGuigan and W. Soldner, *QCD Cosmology from the Lattice Equation of State*, [0810.0265](#).
- [7] P. Castorina, V. Greco and S. Plumari, *Qcd equation of state and cosmological parameters in the early universe*, *Phys. Rev. D* **92** (2015) 063530.
- [8] C. Davies, *Lattice QCD: A Guide for people who want results*, in *58th Scottish Universities Summer School in Physics (SUSSP58): A NATO Advanced Study Institute and EU Hadron Physics 13 Summer Institute*, pp. 233–272, 9, 2005 [[hep-lat/0509046](#)].
- [9] P. Boyle et al., *Lattice QCD and the Computational Frontier*, in *2022 Snowmass Summer Study*, 3, 2022 [[2204.00039](#)].
- [10] HOTQCD collaboration, *The QCD crossover at zero and non-zero baryon densities from Lattice QCD*, *Nucl. Phys. A* **982** (2019) 847 [[1807.05607](#)].
- [11] S. Borsanyi, Z. Fodor, J.N. Guenther, R. Kara, S.D. Katz, P. Parotto et al., *QCD Crossover at Finite Chemical Potential from Lattice Simulations*, *Phys. Rev. Lett.* **125** (2020) 052001 [[2002.02821](#)].
- [12] HOTQCD collaboration, *Chiral crossover in QCD at zero and non-zero chemical potentials*, *Phys. Lett. B* **795** (2019) 15 [[1812.08235](#)].
- [13] S. Li and H. Ding, *Chiral Crossover and Chiral Phase Transition Temperatures from Lattice QCD*, *Nucl. Phys. Rev.* **37** (2020) 674.
- [14] J.N. Guenther, S. Borsányi, Z. Fodor, R. Kara, S.D. Katz, P. Parotto et al., *The crossover line in the (T, μ) -phase diagram of QCD*, *Nucl. Phys. A* **1005** (2021) 121782.
- [15] S. Gupta, *Lattice QCD with chemical potential: Evading the fermion-sign problem*, *Pramana* **63** (2004) 1211.
- [16] J. Danzer, C. Gatttringer, L. Liptak and M. Marinkovic, *A Study of the sign problem for lattice QCD with chemical potential*, *Phys. Lett. B* **682** (2009) 240 [[0907.3084](#)].
- [17] V.A. Goy, V. Bornyakov, D. Boyda, A. Molochkov, A. Nakamura, A. Nikolaev et al., *Sign problem in finite density lattice QCD*, *PTEP* **2017** (2017) 031D01 [[1611.08093](#)].

- [18] K. Nagata, *Finite-density lattice QCD and sign problem: Current status and open problems*, *Prog. Part. Nucl. Phys.* **127** (2022) 103991 [[2108.12423](#)].
- [19] F. Palumbo, *The Chemical potential in the transfer matrix and in the path integral formulation of QCD on a lattice*, *Nucl. Phys. B* **645** (2002) 309 [[hep-lat/0208002](#)].
- [20] A. Nakamura, Y. Sasai and T. Takaishi, *Finite density lattice QCD: How to fight against the complex fermion determinant*, *AIP Conf. Proc.* **756** (2005) 416.
- [21] S. Ejiri, *Remarks on the multiparameter reweighting method for the study of lattice QCD at nonzero temperature and density*, *Phys. Rev. D* **69** (2004) 094506 [[hep-lat/0401012](#)].
- [22] A. Li, A. Alexandru and K.-F. Liu, *Reweighting method in finite density lattice QCD*, *PoS LAT2006* (2006) 030 [[hep-lat/0612011](#)].
- [23] N. Bilic, H. Gausterer and S. Sanielevici, *Complex Langevin Solution to an Effective Theory of Lattice QCD*, *Phys. Rev. D* **37** (1988) 3684.
- [24] G. Aarts, F. Attanasio, B. Jäger and D. Sexty, *Complex Langevin in Lattice QCD: dynamic stabilisation and the phase diagram*, *Acta Phys. Polon. Supp.* **9** (2016) 621 [[1607.05642](#)].
- [25] J.B. Kogut and D.K. Sinclair, *Applying Complex Langevin Simulations to Lattice QCD at Finite Density*, *Phys. Rev. D* **100** (2019) 054512 [[1903.02622](#)].
- [26] D.K. Sinclair and J.B. Kogut, *Applying Complex Langevin to Lattice QCD at finite μ* , *PoS LATTICE2019* (2019) 245 [[1910.11412](#)].
- [27] AURORASCIENCE collaboration, *New approach to the sign problem in quantum field theories: High density QCD on a Lefschetz thimble*, *Phys. Rev. D* **86** (2012) 074506 [[1205.3996](#)].
- [28] M. Cristoforetti, F. Di Renzo, A. Mukherjee and L. Scorzato, *Monte Carlo simulations on the Lefschetz thimble: Taming the sign problem*, *Phys. Rev. D* **88** (2013) 051501 [[1303.7204](#)].
- [29] L. Scorzato, *The Lefschetz thimble and the sign problem*, *PoS LATTICE2015* (2016) 016 [[1512.08039](#)].
- [30] R.V. Gavai and S. Gupta, *Pressure and nonlinear susceptibilities in QCD at finite chemical potentials*, *Phys. Rev. D* **68** (2003) 034506 [[hep-lat/0303013](#)].
- [31] S. Ejiri, C.R. Allton, S.J. Hands, O. Kaczmarek, F. Karsch, E. Laermann et al., *Study of QCD thermodynamics at finite density by Taylor expansion*, *Prog. Theor. Phys. Suppl.* **153** (2004) 118 [[hep-lat/0312006](#)].
- [32] R.V. Gavai and S. Gupta, *The Critical end point of QCD*, *Phys. Rev. D* **71** (2005) 114014 [[hep-lat/0412035](#)].
- [33] R.V. Gavai and S. Gupta, *QCD at finite chemical potential with six time slices*, *Phys. Rev. D* **78** (2008) 114503 [[0806.2233](#)].
- [34] RBC-BIELEFELD collaboration, *Non-zero density QCD by the Taylor expansion method: The Isentropic equation of state, hadronic fluctuations and more*, *PoS LATTICE2008* (2008) 172 [[0810.0375](#)].
- [35] R. Falcone, E. Laermann and M.P. Lombardo, *Study of finite temperature QCD with 2+1 flavors via Taylor expansion and imaginary chemical potential*, *PoS LATTICE2010* (2010) 183 [[1012.4694](#)].
- [36] M. D'Elia and M.-P. Lombardo, *Imaginary chemical potential in QCD at finite temperature*, in *Workshop on Quark Gluon Plasma and Relativistic Heavy Ions*, 5, 2002, DOI [[hep-lat/0205022](#)].

- [37] M.P. Lombardo, *Lattice QCD at finite density: Imaginary chemical potential*, *PoS CPOD2006* (2006) 003 [[hep-lat/0612017](#)].
- [38] Y. Sakai, K. Kashiwa, H. Kouno, M. Matsuzaki and M. Yahiro, *Determination of QCD phase diagram from the imaginary chemical potential region*, *Phys. Rev. D* **79** (2009) 096001 [[0902.0487](#)].
- [39] Z. Fodor, S.D. Katz and K.K. Szabo, *The QCD equation of state at nonzero densities: Lattice result*, *Phys. Lett. B* **568** (2003) 73 [[hep-lat/0208078](#)].
- [40] Y. Aoki, Z. Fodor, S.D. Katz and K.K. Szabo, *The Equation of state in lattice QCD: With physical quark masses towards the continuum limit*, *JHEP* **01** (2006) 089 [[hep-lat/0510084](#)].
- [41] D.E. Miller, *Lattice QCD Calculation for the Physical Equation of State*, *Phys. Rept.* **443** (2007) 55 [[hep-ph/0608234](#)].
- [42] RBC, HOTQCD collaboration, *Equation of state and more from lattice regularized QCD*, *J. Phys. G* **35** (2008) 104096 [[0804.4148](#)].
- [43] K. Kanaya, *Lattice results on the phase structure and equation of state in QCD at finite temperature*, *AIP Conf. Proc.* **1343** (2011) 57 [[1012.4235](#)].
- [44] P. Huovinen and P. Petreczky, *Equation of state at finite baryon density based on lattice QCD*, *J. Phys. G* **38** (2011) 124103 [[1106.6227](#)].
- [45] O. Philipsen, *The QCD equation of state from the lattice*, *Prog. Part. Nucl. Phys.* **70** (2013) 55 [[1207.5999](#)].
- [46] BNL–BIELEFELD–CCNU collaboration, *The QCD equation of state to $\mathcal{O}(\mu_B^4)$ from lattice QCD*, *Nucl. Phys. A* **931** (2014) 851 [[1408.6305](#)].
- [47] A. Bazavov et al., *The QCD Equation of State to $\mathcal{O}(\mu_B^6)$ from Lattice QCD*, *Phys. Rev. D* **95** (2017) 054504 [[1701.04325](#)].
- [48] G. Cvetič and R. Kogerler, *Applying generalized Padé approximants in analytic QCD models*, *Phys. Rev. D* **84** (2011) 056005 [[1107.2902](#)].
- [49] A. Pásztor, Z. Szép and G. Markó, *Apparent convergence of Padé approximants for the crossover line in finite density QCD*, *Phys. Rev. D* **103** (2021) 034511 [[2010.00394](#)].
- [50] HOTQCD collaboration, *Taylor expansions and Padé approximants for cumulants of conserved charge fluctuations at nonvanishing chemical potentials*, *Phys. Rev. D* **105** (2022) 074511 [[2202.09184](#)].
- [51] S. Mondal, S. Mukherjee and P. Hegde, *Lattice QCD Equation of State for Nonvanishing Chemical Potential by Resumming Taylor Expansions*, *Phys. Rev. Lett.* **128** (2022) 022001 [[2106.03165](#)].
- [52] S. Mitra and P. Hegde, *QCD equation of state at finite chemical potential from an unbiased exponential resummation of the lattice QCD Taylor series*, *Phys. Rev. D* **108** (2023) 034502 [[2302.06460](#)].
- [53] S. Mitra, *Determination of Lattice QCD Equation of state at a finite chemical potential*, [2209.11937](#).
- [54] S. Mitra, P. Hegde and C. Schmidt, *New way to resum the lattice QCD Taylor series equation of state at finite chemical potential*, *Phys. Rev. D* **106** (2022) 034504 [[2205.08517](#)].
- [55] S. Mitra, P. Hegde and C. Schmidt, *A new way to resum Lattice QCD equation of state at finite chemical potential*, *PoS LATTICE2022* (2023) 153 [[2209.07241](#)].

- [56] P. de Forcrand, M.A. Stephanov and U. Wenger, *On the phase diagram of QCD at finite isospin density*, *PoS LATTICE2007* (2007) 237 [[0711.0023](#)].
- [57] J.M. Moller, *On the Phase Diagram of QCD with Small Isospin Chemical Potential*, *Phys. Lett. B* **683** (2010) 235 [[0908.1642](#)].
- [58] B.B. Brandt, G. Endrodi and S. Schmalzbauer, *QCD phase diagram for nonzero isospin-asymmetry*, *Phys. Rev. D* **97** (2018) 054514 [[1712.08190](#)].
- [59] B.B. Brandt and G. Endrodi, *Reliability of Taylor expansions in QCD*, *Phys. Rev. D* **99** (2019) 014518 [[1810.11045](#)].
- [60] H.-P. Ying, *Stochastic estimations of fermion matrix determinants with unbiased subtractions*, *Chin. Phys. Lett.* **15** (1998) 401.
- [61] K. Symanzik, *Continuum Limit and Improved Action in Lattice Theories. 1. Principles and ϕ^{*4} Theory*, *Nucl. Phys. B* **226** (1983) 187.
- [62] K. Symanzik, *Continuum Limit and Improved Action in Lattice Theories. 2. $O(N)$ Nonlinear Sigma Model in Perturbation Theory*, *Nucl. Phys. B* **226** (1983) 205.
- [63] E. Gabrielli, G. Heatlie, G. Martinelli, C. Pittori, G.C. Rossi, C.T. Sachrajda et al., *'Improved' computations in lattice QCD*, *Nucl. Phys. B Proc. Suppl.* **20** (1991) 448.
- [64] MILC collaboration, *HISQ action in dynamical simulations*, *PoS LATTICE2008* (2008) 033 [[0903.0874](#)].
- [65] MILC collaboration, *Scaling studies of QCD with the dynamical HISQ action*, *Phys. Rev. D* **82** (2010) 074501 [[1004.0342](#)].
- [66] HOTQCD COLLABORATION collaboration, *Second order cumulants of conserved charge fluctuations revisited: Vanishing chemical potentials*, *Phys. Rev. D* **104** (2021) 074512.
- [67] C.R. Allton, M. Doring, S. Ejiri, S.J. Hands, O. Kaczmarek, F. Karsch et al., *Thermodynamics of two flavor QCD to sixth order in quark chemical potential*, *Phys. Rev. D* **71** (2005) 054508 [[hep-lat/0501030](#)].
- [68] P. Steinbrecher [HotQCD], *The QCD crossover at zero and non-zero baryon densities from Lattice QCD*, *Nucl. Phys. A* **982** (2019) , 847-850 [[1807.05607](#)].